Published in final edited form as:
Neurobiol Dis. 2012 February ; 45(2): 723–732. doi:10.1016/j.nbd.2011.10.018.

Transcriptional changes in adhesion-related genes are site-specific during noise-induced cochlear pathogenesis

Qunfeng Cai[1], **Minal Patel**[1], **Donald Coling**[1], and **Bo Hua Hu**[1,*]

Qunfeng Cai: qcai@buffalo.edu; Minal Patel: minalpat@buffalo.edu; Donald Coling: dcoling@buffalo.edu; Bo Hua Hu: bhu@buffalo.edu

[1]Center for Hearing and Deafness, State University of New York at Buffalo, 137 Cary Hall, 3435 Main Street, Buffalo, NY 14214, USA

Abstract

Cell-cell junctions and junctions between cells and extracellular matrix are essential for maintenance of the structural and functional integrity of the cochlea, and are also a major target of acoustic trauma. While morphological assessments have revealed adhesion dysfunction in noise-traumatized cochleae, the molecular mechanisms responsible for adhesion disruption are not clear. Here, we screened the transcriptional expression of 49 adhesion-related genes in normal rat cochleae and measured the expression changes in the early phases of cochlear pathogenesis after acoustic trauma. We found that genes from four adhesion families, including the immunoglobulin superfamily and the integrin, cadherin, and selectin families, are expressed in the normal cochlea. Exposure to an intense noise at 120 dB sound pressure level (SPL) for 2 h caused site-specific changes in expression levels in the apical and the basal sections of the sensory epithelium. Expression changes that occurred in the cochlear sensory epithelium were biphasic, with early upregulation at 2 h post-noise exposure and subsequent downregulation at 1 day post-exposure. Importantly, the altered expression level of seven genes (*Sgce*, *sell*, *Itga5*, *Itgal*, *Selp*, *Cntn1* and *Col5a1*) is related to the level of threshold shift of the auditory brainstem response (ABR), an index reflecting functional change in the cochlea. Notably, the genes showing expression changes exhibited diverse constitutive expression levels and belong to multiple adhesion gene families. The finding of expression changes in multiple families of adhesion genes in a temporal fashion (2 h vs. 1 day) and a spatial fashion (the apical and the basal sensory epithelia as well as the lateral wall tissue) suggests that acoustic overstimulation provokes a complex response in adhesion genes, which likely involves multiple adhesion-related signaling pathways.

Keywords

Cochlea; Sensory epithelium; Hair cells; Acoustic trauma; Adhesion; Transcriptional expression; Noise

[*]Corresponding author: Bo Hua Hu, Ph.D., Center for Hearing and Deafness, State University of New York at Buffalo, 137 Cary Hall, 3435 Main Street, Buffalo, NY 14214, USA, Phone: 1-716-829-5316, Fax: 001-716-829-2980, bhu@buffalo.edu.

Introduction

Acoustic overstimulation is a common cause of acquired sensorineural hearing loss in the adult population. There is considerable evidence that functional loss of the cochlea is not simply a consequence of the initial mechanical destruction of the cochlea, but is also attributed to the development of complex secondary events that contributed to early as well as delayed cell damage. Gaining an understanding of the molecular mechanisms underlying cochlear damage is an important step in developing therapeutic strategies for the prevention of noise-induced hearing loss.

Cell adhesion is essential for maintenance of tissue integrity. Excessive movement of the basilar membrane of the cochlea due to acoustic overstimulation stretches the organ of Corti and compromises both cell-cell junctions and adhesion of cells to extracellular matrix. Morphological evidence for structural disruption of intercellular junctions has been observed in animal models of acoustic trauma (Hamernik et al., 1984; Henderson and Hamernik, 1986; Lim and Melnick, 1971; Saunders et al., 1985; Thorne et al., 1984), while alteration in the barrier function of the reticular lamina due to cell junction dysfunction has also been observed (Hu and Zheng, 2008).

Cell adhesion in the mammalian organ of Corti relies on the function of tight junctions, gap junctions, adherens junctions, and desmosomes (Gulley and Reese, 1976; Kikuchi et al., 2000; Nadol, 1978; Raphael and Altschuler, 1991), as well as focal adhesions that form junctions between cells and extracellular matrix (Jamesdaniel et al., 2011; Littlewood Evans and Muller, 2000; Meyer zum Gottesberge et al., 2008; Tian et al., 2009). These junctions work coherently to maintain functional and structural integrity of tissues. Gap junctions are intercellular channels that facilitate direct communication of ions and small cytoplasmic molecules. In the cochlear sensory epithelium, gap junctions are distributed between supporting cells (Forge et al., 1999; Kikuchi et al., 1995), and mutation of gap junction genes has been linked to congenital hearing loss (Nickel and Forge, 2008). The tight junction is responsible for establishing compositionally distinct compartments by forming tight seals between cells (Anderson and Van Itallie, 1995; Schneeberger and Lynch, 1992). In the cochlea, the tight junction is important for maintenance of the barrier function of the reticular lamina (Gulley and Reese, 1976), and mutation of tight junction-associated genes causes hearing loss(Riazuddin et al., 2006; Wilcox et al., 2001). The adherens junction is present in both sensory cell and supporting cell junctions (Leonova and Raphael, 1997; Nunes et al., 2006). In the reticular lamina, adherens junction proteins are intermingled with the tight junction proteins, forming a hybrid tight junction that encircles the cells (Nunes et al., 2006). Adherens junction proteins also play an important role in maintaining the structural integrity of the cytoskeleton. Alteration of adherens proteins, such as cadherins, leads to disruption of the actin structure of cells (Tsukita et al., 1992).

Thus far, only a handful of adhesion-related molecules have been identified and their distributions in the cochlea documented (Davies and Holley, 2002; Simonneau et al., 2003; Suzuki and Harris, 1995; Toyama et al., 2005; Tsuprun and Santi, 1999; Whitlon and Rutishauser, 1990). These molecules belong to multiple adhesion gene families, including the immunoglobulin superfamily and the integrin and cadherin families. The involvement of adhesion molecules has been implicated in scar formation in the organ of Corti during the recovery phases of acoustic injury (Raphael and Altschuler, 1991). A recent study has shown that mice lacking the vezatin protein, a ubiquitous adherens junction protein, exhibit a high vulnerability to acoustic trauma (Bahloul et al., 2009), suggesting that this adherens junction gene regulates sensory cell responses to acoustic overstimulation. Although these studies have linked adhesion genes to noise-induced cochlear pathogenesis, our understanding of adhesion signaling pathways in cochlear pathogenesis remains limited.

In non-cochlear tissues, adhesion proteins have been implicated in mediating signaling pathways in various pathological conditions, including cell detachment (Frisch and Screaton, 2001; Grossmann, 2002; Haga et al., 2008; Malik, 1997). The detachment of cells from their anchorage has been shown to be a trigger for apoptosis (Frisch, 2000). For example, Frisch and Francis (Frisch and Francis, 1994) reported that disruption of normal epithelial cell–matrix interactions in culture resulted in apoptotic cell death. Because noise exposure stretches the basilar membrane and compromises cell-cell junctions, we suspected that acoustic trauma could alter adhesion molecule expression, which in turn could affect cell survival. One unresolved question is which adhesion-related genes participate in the early response of adhesion junctions to acoustic trauma, a possible early event in acute sensory cell death (Hu et al., 2006).

The mammalian cochlea consists of three major partitions: the sensory epithelium, the lateral wall, and the modiolus, each playing a distinct role in maintaining cochlear function. While the modiolus is protected by a bony shell, the sensory epithelium and the lateral wall tissue can sustain direct mechanical insult, and morphological observations have identified the sensory epithelium as the primary site of acoustic injury (Henderson and Hamernik, 1986; Saunders et al., 1985). In the sensory epithelium, the basal and the apical partitions differ in several ways. Anatomically, the basilar membrane is narrower, and sensory cells are smaller in the basal end. Physiologically, the cochlea is organized in a tonotopic manner, with lower frequencies encoded at the apical end and higher frequencies encoded at the basal end. The two partitions of the sensory epithelium differ also in certain biological properties. For example, the expression of certain genes exhibits a basal-to-apical gradient in the sensory epithelium (Weston et al., 2011). Functionally, the basal end exhibits less antioxidant capacity, and is prone to oxidative stress (Sha et al., 2001), while basal sensory cells exhibit a higher susceptibility to ototoxicity and age-related degeneration (Fechter et al., 1997; Forge and Schacht, 2000; Sha et al., 2001). Importantly, previous investigations have demonstrated a greater vulnerability to acoustic injury in the basal sensory cells (Bohne et al., 1987; Hu et al., 2002b; Pouyatos et al., 2009; Thorne et al., 1984). These spatial differences in the properties of the sensory epithelium prompted us to investigate site-specific changes in the expression levels of adhesion-related genes.

In the current investigation, we examined the expression patterns of 49 adhesion-related genes in three cochlear partitions (the apical and the basal sections of the sensory epithelium and the lateral wall tissues) in normal and noise-traumatized rat cochleae. This study identified the expression of several adhesion-related genes, many of which have not been reported for cochlear tissues. This study also documents noise-induced differential changes in the expression pattern of the adhesion genes and reveals a significant correlation between the expression levels of certain adhesion genes and loss of the cochlear function. These results provide important clues for the understanding of adhesion signaling pathways in noise-induced cochlear pathogenesis.

Materials and Methods

Animals

Sasco Sprague Dawley rats (2–4 months old, 210–300g, male and female, Charles River Laboratories, Wilmington, MA) were used in the current study. All animals received a baseline-hearing test. Only the animals with normal hearing sensitivity were included in the study. The procedures involving use and care of the animals were reviewed and approved by the State University of New York at Buffalo Institutional Animal Care and Use Committee.

Experimental Design

All animals received a baseline ABR test, and were then randomly assigned to either a normal control group (without receiving noise exposure) or a noise group. The noise group animals were exposed to intense noise for 2 h. The exposed animals were sacrificed after the final ABR test at either 2 h or 1 day post-exposure. Additional four animals were allowed to survive for 28 days for evaluation of permanent hearing loss. For the animals that were sacrificed at 2 h after noise exposure, one cochlea from each animal was used for assessment of mRNA expression levels of adhesion-related genes and the other cochlea was used for assessment of sensory cell damage. Five additional animals from the noise group were used for the analysis of Cdh1 protein expression. The separate experimental procedures are detailed below.

Noise Exposure

A continuous noise (1–7 kHz) for 2 h at 120 dB sound pressure level (re 20μPa) was used to induce acoustic trauma to the cochlea. The noise signal was generated with a real-time signal processor (RP2.1; TDT, Alachua, FL, USA). The signal was routed through an attenuator (PA5; TDT) and a power amplifier (Crown XLS 202; Harman International Company, China) to a loud speaker (NSD2005–8; Eminence). The noise level was calibrated using a sound level meter (Larson Davis 800 B; Depew, NY, USA), a preamplifier (Larson and Davis; model 825), and a condenser microphone (Larson and Davis; LDL 2559) that was placed at the position of the animals head in the sound field. The rats were individually exposed to the noise in a holding cage to ensure a consistent level of noise exposure.

Auditory Brainstem Response (ABR) test

ABR measurements were conducted pre- and three times post-exposure (2 h, 1 day and 28 days) to determine the hearing sensitivity of the animals. ABRs were recorded as previously described (Hu et al., 2009). Briefly, an animal was anesthetized with intraperitoneal injection of a mixture of ketamine (87 mg/kg) and xylazine (3 mg/kg). The body temperature was maintained at 37.5°C with a warming blanket (Harvard Apparatus). Stainless-steel needle electrodes were placed subdermally over the vertex (noninverting input) and posterior to the stimulated and nonstimulated ear (inverting input and ground) of the animal. ABRs were elicited with tone bursts at 5, 10, 20, 30, and 40 kHz (0.5 msec rise/fall Blackman ramp, 1 msec duration, alternating phase) at the rate of 21/sec, which were generated digitally (SigGen; TDT) using a D/A converter (RP2.1; TDT; 100 kHz sampling rate) and fed to a programmable attenuator (PA5; TDT), an amplifier (SA1; TDT), and a closed-field loudspeaker (CF1; TDT). The electrode outputs were delivered to a pre-amplifier (RA4LI and RA4PA; TDT) and then to a medusa base station (RA16BA, TDT). Responses were filtered (100–3000 Hz), amplified (20×) and averaged using TDT hardware and software. These responses were then stored and displayed on a computer. The ABR threshold was defined as the lowest intensity that reliably elicited a detectable response.

Assessment of sensory cell damage

The organs of Corti were isolated for pathological examination 2 h post-exposure using a method that has been described in our previous publication (Hu and Cai, 2010). Propidium iodide (Invitrogen Inc.) was used as a nuclear marker to stain the cochleae for assessment of cell damage. Briefly, 2 h after noise exposure the animal was deeply anesthetized and decapitated. The cochlea (either right or left) was quickly removed from the skull, and perfused with a propidium iodide solution (5 μg/ml in 10 mM phosphate buffered saline, PBS) for 10 min. The cochlea was then perfused with 10 mM PBS to remove the propidium iodide solution and then fixed with 10% buffered formalin for at least 4 h. After dissection,

the organ of Corti was collected and mounted on a slide with an antifade medium (Prolong® Gold antifade reagent, Invitrogen. Inc.).

To confirm that sensory cells showing condensed or fragmented nuclei were dying via the apoptotic pathway, caspase-3 activity, a biological marker of apoptosis, was detected using a fluorescent probe, FAM-DEVD-FMK (APT403; Millipore, Bedford, MA). The basic procedure for caspase-3 labeling has been described in detail in our previous publication (Hu and Cai, 2010). Briefly, the animals were scarified at 2 h post-noise exposure. The cochleae were quickly collected and perfused with approximately 20 μl of the freshly prepared staining solution diluted according to the manufacturer's instructions. The staining solution remained in the cochlea for 50 min, and then the cochlea was fixed with 10% buffered formalin. After dissection, the organs of Corti were further stained with propidium iodide for 10 min.

The specimens were examined with a fluorescence microscope to identify hair cell lesions. The pathological criteria used for identifying damaged cells have been previously described (Hu et al., 2002b; Yang et al., 2004). Based on the nuclear morphology, the numbers of damaged and missing hair cells were identified and counted. The data were assembled into a cochleogram showing the frequency-place correlation for the rat (Muller, 1991).

mRNA expression levels of adhesion-related genes

We assessed the expression levels of 49 adhesion-related genes using PARN-013A SABiosciences adhesion arrays (Qiagen, Valencia, CA) (see Table 1 for the gene list). Methodology to isolate total RNA, synthesize and pre-amplify cDNA and run qRT-PCR reactions was performed as previously described (Hu and Cai, 2010; Hu et al., 2009). Briefly, the animal was decapitated and either the left or the right cochlea was quickly removed from the skull. The cochlea was perfused with an RNA stabilization reagent (RNAlater; Qiagen, Valencia, CA), and was dissected in the same reagent. Three samples (the apical and the basal sensory epithelium as well as the lateral wall tissue) were collected from the cochlea. The apical sample contained the apical 45% of the sensory epithelium and the basal sample contained the tissue from 45% to 90% from the apex of the sensory epithelium. The lateral wall sample consisted of the lateral wall tissue from the second cochlear turn. Each sample was run separately for qRT-PCR analysis. Total RNA was isolated from each sample using the RNeasy Micro Kit (Qiagen) as per manufacturer's instruction. The concentration of isolated total RNA was measured with a NanoDrop instrument (NanoDrop 1000, Thermo Scientific). The isolated total RNA was used to generate cDNA and the cDNA was pre-amplified using the RT^2 Nano PreAMP cDNA Synthesis Kit (Qiagen). Synthesized cDNA was mixed with RT^2 Real-Time PCR SYBR Green/Fluorescein Master Mix (Qiagen) and transferred to a 96-well plate. qRT-PCR was performed using a Bio-Rad MyiQ Single-Color Real-Time PCR System. At least four biological repetitions were performed for each experimental condition.

The quality control of mRNA quantification was performed using three integrated control assays in the PCR array: the reverse transcription control, positive PCR control, and genomic DNA control. All PCR runs passed the first two control tests. However, the DNA contamination analysis identified one array to be contaminated by genomic DNA. As a result, the data from this array were excluded from the final analysis.

Immunohistology

Immunohistochemistry was used to localize protein expression of Cdh1 in the organ of Corti. The control (without receiving noise exposure) and the noise-traumatized animals were sacrificed. The cochleae were fixed with 10% buffered formalin and organs of Corti

were dissected. Dissected tissues were then permeabilized for 30 min with 0.2% Triton X-100 in 10 mM PBS, blocked using 10% goat serum in PBS and then incubated with purified mouse E-cadherin primary antibody (1:200, BD Biosciences) at 4°C overnight. The tissues were then rinsed with 10 mM PBS (3×), incubated with a secondary antibody (Alexa Fluor 488 goat anti-mouse, 1:500, Invitrogen) for 1 h and then counterstained with propidium iodide. Two additional organs of Corti, one from a control subject and one from a noise-traumatized subject, were stained with only the secondary antibody to assess nonspecific staining.

Data analyses

ABR measurements—A two-way ANOVA (post-exposure time × test frequency) was used to compare ABR threshold shifts measured at 2 h, 1 day and 28 days post-exposure and among the five tested frequencies. If a significant main effect occurred, post hoc testing with a Tukey test was performed to delineate the nature of the differences.

Sensory cell damage—All the specimens were observed with a fluorescence microscope to identify cochlear lesions, which were further observed with a confocal microscope (Zeiss LSM510 multichannel laser scanning confocal imaging system) using a method that has been reported previously (Hu et al., 2006). To determine the site of primary lesions, we divided the sensory epithelium into the apical section and the basal section. The apical section contained the apical 45% sensory epithelium and the basal section consisted of the sensory epithelium section 45% to 90% from the apex. A paired Student's t test was performed to compare the numbers of damaged sensory cells between the apical and the basal section of the sensory epithelia. An α level of 0.05 was selected for significance.

Quantification of Cdh1 positive sensory cells—The numbers of Cdh1-positive sensory cells in the apical and the basal sensory epithelium sections were quantified by counting the sensory cells exhibiting strong Cdh1 immunoreactivity in their top junctions with supporting cells. The numbers were compared using a paired Student's t test. An α level of 0.05 was selected for significance.

Analyses of mRNA expression levels of adhesion-related genes—The raw Ct value of each gene was first normalized to reference genes. The reference genes were selected from the five housekeeping genes (*Rplp1, Hprt1, Rpl13a, Ldha and Actb*) that are integrated into the qRT-PCR array. We used geNorm software to calculate the internal control gene-stability measures (M value) (Vandesompele et al., 2002), a quantitative parameter for the assessment of expression level variation of reference genes. Based on the M value, we selected three most stable genes (*Rplp1, Hprt1 and Actb*) and used the arithmetic mean of their expression levels as the baseline to calculate the ΔCt of each targeted gene. The fold changes in the expression levels of adhesion-related genes were calculated across two groups as $\Delta\Delta Ct = \Delta Ct$ (noise group) − ΔCt (control group). The significance of the changes was analyzed using SAM (Significance Analysis of Microarrays) (Tusher et al., 2001) with the number of permutation of 100. A significant change was defined as *q*-values less than or equal to 0.01 and fold differences equal to or greater than 2. Because a Ct value of 35 represents single molecule template detection (Guthrie et al., 2008), a gene expression level with the raw Ct value greater than 35 was considered to be below the detection level of the assay in the current investigation.

Results

Expression patterns of adhesion genes in the apical and basal sections of the normal sensory epithelium

To profile the expression pattern of adhesion-related genes under normal conditions, we examined the constitutive expression levels of 49 adhesion-related genes in the apical and the basal sections of the sensory epithelium and found diverse expression levels of these genes (Supplementary Table S1). The highest-expressed genes (*Ctnnb1, Catna1, Thbs1,* and *Lamb2*) had expression levels either greater or less than, but within 1 cycle difference of, the average expression level of the reference control genes. The lowest-expressed genes (*Sele, Itgad, Itgae,* and *Sell*) had raw Ct values of >35 or were undetectable.

Anatomically, the apical and the basal sections of the sensory epithelium have the same cell populations, yet they differ in many ways in their physiological and biological characteristics. We therefore sought to determine whether these two sections have different expression patterns for adhesion genes. First, we calculated the Pearson's correlation coefficient of the ΔCt values across the 49 genes and found that the ΔCt values of the genes are highly correlated between the two partitions ($r = 0.95$, $p < 0.0001$ and slope = 1.007, Fig. 1). However, certain genes appeared to be less coordinated in their expression. To define the difference, we examined the fold differences in gene expression level using the SAM algorithm. Among the 49 examined genes, four were more highly expressed in the apical sections, whereas 23 were more highly expressed in the basal sections, with fold differences ranging from 2.55 to 14.35 and a false discovery rate <0.015 (bar graph in Fig. 2). To further illustrate the difference, we ranked the 49 genes based on their expression levels and compared the rank positions of the genes between the two anatomic sites. We found differences in the rank positions for multiple genes (scatter plot in Fig. 2). Notably, the result of the rank analysis is consistent with the result of the fold-difference analysis. Together, these observations suggest that transcriptional expression patterns of adhesion-related genes are not completely parallel in the apical and basal sections of the cochlear sensory epithelium.

Exposure to intense noise causes both functional deterioration and sensory cell damage in the cochlea

Exposure to intense noise traumatizes cochlear structures. To provide the cochlear damage context for profiling the gene expression levels, we examined the functional and morphological changes of the cochleae following the acoustic trauma. ABRs were measured pre-exposure and at three time points post-exposure (2 h, 1 day, and 28 days). Threshold shifts obtained at the first two post-exposure time points represent temporary threshold shifts, while threshold shifts measured at the last time point represent the permanent threshold shifts. Figure 3A shows the pre- and post-exposure ABR thresholds at the five tested frequencies representing low-, middle-, and high-frequency hearing. The analysis of post-exposure threshold shifts with a two-way ANOVA (time × frequency factors) revealed a significant effect of time ($F = 233.06$; df 2,145; $p < 0.001$) and a significant effect of frequency ($F = 31.63$; df 4,145; $p < 0.01$). The elevation of the thresholds was evident at 2 h post-exposure, with an average threshold shift of 70.1 ± 16.0 dB (mean ± SD). The frequency dependence of the threshold shifts was relatively flat, with slightly greater loss in the low frequencies (5 and 10 kHz, both differ from other frequencies, Tukey test, $p < 0.001$) and a notch at 20 kHz (differing from all other frequencies, Tukey test, $p < 0.001$). The thresholds were partially recovered at 1 day post-exposure (Tukey test, $p < 0.001$) and further recovered at 28 days post-exposure (Tukey test, $p < 0.001$), leaving an average permanent threshold shift of 23.1 ± 14.6 dB (mean ± SD). This observation suggests that the

noise level used in the current investigation was capable of inducing a permanent loss of hearing sensitivity.

To further evaluate the impact of noise, we examined the level of sensory cell damage at 2 h post-exposure. Nuclear morphology was used as the index for defining sensory cell damage, because its change is an early sign of damage and because its progression occurs in a step-by-step fashion (Hu et al., 2006; Yang et al., 2004). We found malformed sensory cell nuclei, as well as indications of missing cells, at this time point (Fig. 3B). Caspase-3 staining revealed that sensory cells having condensed or fragmented nuclei exhibited strong caspase-3 activity (Fig. 3C), suggesting that these cells were apoptotic cells. In contrast, the malformed or missing nuclei were rare in normal control ears (Fig. 3D). To quantify the level of damage, we counted the damaged cells (the cells with condensed or swollen nuclei, as well as missing cells) along the entire length of the organs of Corti and used the data to assemble a cochleogram. As shown in Figure 3E, there were two lesions in the organ of Corti, one in the apical partition and the other in the basal partition of the cochlea. We then compared the numbers of total damaged cells between the apical and the basal sections and found that the basal partition had more damaged cells (22.3 ± 27.6 vs. 62.1 ±64.8, mean ± SD; paired Student's t test, $p = 0.003$, Fig. 3F), suggesting that the basal section is the major site of sensory cell pathogenesis. Notably, the noise-induced damage was significantly greater than the spontaneous sensory cell degeneration in normal cochleae (22.3 ± 27.6 vs. 2.9 ± 3.4 for the apical partition; 62.1 ± 64.8 vs. 16.9 ± 13.4 for the basal partition; Student's t test, $p = 0.01$ for both partitions). Together, these observations indicate that the noise condition used in the current study was capable of inducing not only hearing loss but also sensory cell death. As shown in our previous publications (Hu and Cai, 2010; Hu et al., 2009), this initial sensory cell damage will continue to develop at 1 day and 7 days post-noise exposure.

Acoustic overstimulation causes a site-specific change in mRNA expression levels of adhesion genes in the sensory epithelium

To define the transcriptional responses of the adhesion-related genes to acoustic overstimulation, we analyzed the fold change in expression level of the 49 genes using SAM software. In the apical samples, five genes (*Sell*, *Thbs1*, *Itgae*, *Icam1*, and *Itga5*) were significantly upregulated and none was downregulated at 2 h post-exposure (Table 2). These upregulated genes belong to different adhesion families, including the immunoglobulin superfamily (*lcam1*) and the selectin (*Sell*) and integrin (*Itgae* and *Itga5*) families. Among these upregulated genes, two (*Sell* and *Itgae*) were undetectable in the normal sensory epithelium, but became detectable after noise exposure.

The basal samples also featured an upregulation of the gene expression level. However, the expression changes in the basal samples were not completely parallel to the apical samples. First, the total number of altered genes was more in the basal partition than in the apical partition (8 genes vs. 5 genes). Second, changes in expression at the two sites involved different gene sets. Three genes (*Itgae*, *Itga5*, and *Sell*) were upregulated in the apical partition, but not in the basal partition. Six genes (*Itga3*, *Itgb2*, *Selp*, *Sele*, *Cdh1*, and *Cdh2*) were upregulated in the basal partition, but not in the apical partition. At this time point, only two genes (*Icam1* and *Thbs1*) co-varied in the two anatomic sites. Together, these data provide evidence that acoustic trauma provokes differential expression changes in adhesion-related genes between the apical and the basal sections of the sensory epithelium.

The site-specific transcriptional change in Cdh1 is consistent with its protein expression change

To provide further evidence for the site-specific response of adhesion genes to acoustic overstimulation in the sensory epithelium, we examined the protein expression of *Cdh1* gene, because this gene had exhibited a significant transcriptional increase only in the basal samples (fold change = 2.46, q = 0 for the basal samples vs. fold change = 1.15, q = 0.47 for the apical samples). Employing immunohistology to identify the protein expression pattern, we found that in the normal cochlear sensory epithelium, strong immunoreactivity to the Cdh1 protein appeared in the intercellular junctions among supporting cells, including Deiters cells, pillar cells and Hensen cells (Fig. 4A), while staining in the junctions around sensory cells was weak or undetectable (data not shown). This finding is consistent with the previously reported distribution of the Cdh1 protein (Nunes et al., 2006; Whitlon, 1993).

After exposure to intense noise, a marked increase in Cdh1 immunoreactivity appeared in some of the outer hair cells in the damaged regions of the sensory epithelium. The fluorescence was located in the circumferential rings of the outer hair cells, the site where the outer hair cell forms junctions with the phalangeal processes of Deiters cells and pillar cells (Figs. 4B and 4C). To determine the viability of these Cdh1-positive cells, we counterstained the tissues with propidium iodide, a nuclear dye, to illustrate nuclear morphology. Most Cdh1-positive cells exhibited malformed nuclei with increased propidium iodide fluorescence, suggesting that these Cdh1-positive cells were damaged (Fig. 4B). However, some Cdh1-positive cells (less than 5% of total Cdh1-positive cells) showed a relatively normal nuclear morphology (Fig. 4C). This may suggest that the change in Cdh1 protein precedes nuclear degradation. Moreover, the result indicates that the site-specific upregulation in Cdh1 expression is spatially correlated with sensory cell degeneration.

To quantify the expression change, we counted the numbers of Cdh1-positive cells in the sensory epithelia, and compared their numbers between the apical and the basal sections. As shown in Figure 4D, the number of Cdh1-positive cells in the basal partition is significantly higher than that in the apical partition (75.5 ± 67.6 vs. 34.7 ± 34.6, mean ± SD, paired Student's t test, $p < 0.01$). This finding is consistent with the observation of significant transcriptional upregulation of *Cdh1* in the basal samples of the sensory epithelia, further suggesting the occurrence of site-specific alteration in expression of adhesion genes.

To verify the specificity of the immunolabeling, we checked the molecular weight of the protein targeted by the Cdh1 antibody using a western blotting assay and found two bands, 100 kDa and 120 kDa, consistent with the molecular weights of the two isoforms of the Cdh1 protein reported in non-cochlear tissues (Barshishat et al., 2000). Moreover, the primary antibody control observation, which omitted the primary antibody, exhibited no fluorescence at the cell-cell junctions in the organ of Corti (date not shown).

Individual variation in the functional loss of the cochleae is correlated with the expression levels of adhesion-related genes

Individual variation in cochlear responses to acoustic trauma has been reported in previous studies (Hunter-Duvar, 1977; Lipscomb et al., 1977; Saunders et al., 1985; Thorne et al., 1984). Given the finding of individual variation in transcriptional levels of adhesion-related genes, we sought to determine whether individual variation in transcription level is related to the level of hearing loss. To this end, we calculated the Pearson's correlation between the average ABR threshold shift and the expression level for each gene. In the apical partition, two genes had expression levels that were correlated with the magnitude of hearing loss, one positively (*Sgce*) and the other negatively (*Sell*), with the positive correlation meaning that a

higher expression level was associated with greater hearing loss (Fig. 5, r = 0.95 and −0.98, respectively, $p < 0.05$). In the basal partition, six genes showed expression levels that were correlated, four positively (*Itga5, Itgal, Sell,* and *Selp*) and two negatively (*Cntn1* and *Col5a1*), with the level of hearing loss (Fig. 5, r = 0.97, 0.95, 0.97, 0.98, −0.99, and −0.96, respectively, $p < 0.05$). We suspect that these genes contribute to an individual's susceptibility to acoustic trauma.

Expression changes occur in genes with diverse baseline levels of expression

Given the diversity of the constitutive expression levels of the 49 genes examined, we wondered whether the baseline transcriptional level of a gene contributes to its propensity to respond to mechanical stress. To address this question, we examined the rank distribution of the expression-altered genes among the 49 genes. The rank position of a gene was based on its constitutive expression level. As shown in Figure 6, the expression-altered genes are spread across the full range of the rank order, indicating that these genes have different constitutive expression levels.

The early transcriptional changes in adhesion-related genes are biphasic

Previous observations have revealed the dynamic nature of cochlear pathogenesis (Hu et al., 2002b; Pye, 1981; Thorne and Gavin, 1985; Yang et al., 2004). We therefore sought to determine whether the early expression change observed at 2 h post-exposure persists to 1 day post-exposure. In contrast to the up-regulation-dominated changes at 2 h post-exposure, the expression pattern at day 1 featured a trend of down-regulation. All the upregulated expression levels observed at 2 h post-exposure returned to their baseline levels. At 1 day post-exposure (Fig. 7), six genes (*Cd44, Pecam1, Ctgf, Ctnna2, Lama2,* and *Cntn1*) were significantly downregulated with fold-changes ranging from 2.47 to 8.29 (SAM analysis, $q = 0$). None of these downregulated genes was upregulated at 2 h post-exposure. The data obtained from the two time points demonstrate the presence of a biphasic change in the expression levels of adhesion-related genes in the first post-exposure day, indicating that the noise-induced transcriptional change is a time-dependent event.

Noise-induced transcriptional changes in the lateral wall tissue of the cochlea

The lateral wall tissue, consisting of the stria vascularis and the spiral ligament, plays an important role in maintaining cochlear function. Although the sensory epithelium is the primary target of acoustic trauma, functional and morphological changes have been found in the lateral wall structures (Engstrom and Engstrom, 1979; Lim, 1976; Shi and Nuttall, 2007). To determine whether acoustic overstimulation causes a parallel change in adhesion gene expression in the lateral wall tissue, we profiled the lateral wall expression of adhesion-related genes and examined their changes at 2 h post-exposure. In contrast to the upregulation-dominated changes in the sensory epithelium, the lateral wall samples featured a downregulation-dominated change in gene expression (Table 3). Among the 25 genes with expression changes, 21 were downregulated, and only four were upregulated. Among the four upregulated genes, three (*Sele, Selp,* and *Thbs1*) co-varied in the sensory epithelium. In contrast, only one gene (*Cdh2*) among the 21 downregulated genes co-varied in the cochlear sensory epithelia. These observations suggest that these upregulated genes (*Sele, Selp,* and *Thbs1*) are more likely to co-vary in the lateral wall and the sensory epithelium, whereas the downregulated genes (see Table 3) tend to be site-specific. Together, our current investigation indicates that exposure to intense noise causes site-specific changes in the sensory epithelium and the lateral wall tissue.

Discussion

The objectives of the current investigation were to profile the transcriptional pattern of adhesion-related genes and to define their expression changes induced by acoustic trauma in the rat cochlea. This study documents the constitutive expression of multiple adhesion-related genes in normal cochlear tissues, many of which have not been previously reported, and also documents noise-induced differential changes in the expression levels of these genes and a high correlation between the expression levels of certain adhesion genes and functional loss of the cochlea. These results provide important clues for further investigation of adhesion signaling pathways in noise-induced cochlear pathogenesis and the repair process.

The effort to understand transcriptional changes in different cochlear partitions, particularly in the different sections of the sensory epithelium, has been hampered by the scarceness of cochlear tissues available for RNA analyses and the difficulty of dissecting fresh cochlear tissues without contamination. Our method, using a combination of the techniques of fresh tissue dissection, cDNA pre-amplification, and RNA preservation, allowed us, for the first time, to investigate site-specific transcriptional changes in the cochlea and to correlate the transcriptional changes to functional change in the cochlea.

We demonstrate in the current study that the constitutive expression levels of certain adhesion-related genes differ in the apical and the basal sections of the sensory epithelium. We also present evidence of a site-specific change in adhesion-gene transcription after exposure to intense noise. Specifically, the apical and the basal samples exhibit different numbers of genes that are altered in expression level. Three genes show expression changes exclusively in the apical samples and six in the basal samples. Only two genes were co-regulated in both the apical and the basal samples. This observation suggests that the apical and basal sections of the sensory epithelium undergo different adhesion modulation with the basal section sustaining a greater adhesion change. This difference may also be attributed to the difference in the damage levels in the two sections of the sensory epithelium. Notably, analyses of gene families show that the site-specific change involves genes from the integrin, cadherin, and selectin gene families, whereas the change in the immunoglobulin family member (*Icam1*) is ubiquitous in the sensory epithelium.

Individual variation in the levels of functional and pathological changes is a hallmark of acoustic trauma (Hunter-Duvar, 1977; Lipscomb et al., 1977; Saunders et al., 1985; Thorne et al., 1984; Wagner et al., 2003), and is clearly evident in the current investigation. However, the molecular basis for the variation is not clear. Our correlation analysis identified seven genes showing a correlation between the expression level and the level of hearing loss. These genes may contribute to the individual variation in the levels of cochlear damage after acoustic overstimulation. However, due to the limited sample size and the limitation of the correlation analysis for defining causality, it is essential to confirm the current results using experimental approaches to manipulating gene expression, so that the roles of these genes in the development of cochlear damage can be more accurately defined.

Cochlear tissues consist of heterogeneous cell populations and the junctions connecting these cells involve multiple adhesion proteins. Previous studies have identified some of the adhesion-related proteins in cochlear tissues, such as proteins from the Cdh1, I-CAM, and integrin families (Davies and Holley, 2002; Suzuki and Harris, 1995; Toyama et al., 2005; Whitlon, 1993). The current study confirms the cochlear expression of the corresponding genes at the transcriptional level. Importantly, we have detected the expression of many genes that have not previously been linked to cochlear structures.

We found expression changes in all four adhesion gene families. Selectin family members are a family of transmembrane molecules that are expressed on the surface of leukocytes and activated endothelial cells (Chen and Geng, 2006; Stamenkovic, 1995). In the current study, we demonstrate that the constitutive expression of selectin family genes (*Sell, Sele,* and *Selp*) is either very low or undetectable, suggesting that these genes may not be major players in the adhesion functions of cochlear structures. However, the expression levels of this gene family were upregulated after noise exposure. Although the biological role of selectin gene activation in cochlear pathogenesis remains unclear, evidence suggests that these genes play an important role in cochlear inflammation. Selectin family members have been found to participate in the inflammatory response by mediating the interaction between leukocytes, platelets, and endothelia (Grailer et al., 2009). In the cochlea, recruitment of inflammatory cells to the injured cochlea has been found after acoustic trauma (Fredelius and Rask-Andersen, 1990; Hirose et al., 2005). We therefore suggest that selectin family genes are mediators of cochlear inflammation. It is likely that controlling expression of these inflammatory genes will serve as a new therapeutic target for suppression of inflammatory responses (Rossi and Constantin, 2008).

We found upregulation of three cadherin family members after acoustic overstimulation. Cadherin proteins are a group of calcium-dependent proteins playing an important role in maintaining cell-cell junction function and cellular architecture via interaction with actin molecules through catenin proteins (Leckband and Prakasam, 2006). Expression of cadherin family genes, including *Cdh1* and *Cdh2*, in the cochlear tissues has been reported (Simonneau et al., 2003; Whitlon, 1993; Whitlon et al., 1999). Thus far, the precise role of the Cdh1 protein in sensory cell degeneration is not clear. Evidence from the current investigation and from previous publications suggests that this protein may be involved in both degenerative and repair processes. In noise-traumatized cochleae, the Cdh1 protein has been implicated in scar formation in the recovery phase of cochlear pathogenesis (Raphael and Altschuler, 1991). Our current investigation further links cadherin family genes to the initial phase of cochlear damage. We found that most sensory cells showing strong Cdh1 immunoreactivity have malformed nuclei. Notably, certain cells with strong Cdh1 immunoreactivity exhibit relatively normal nuclear morphology, suggesting that Cdh1 is involved in the early stages of the degenerative process in these cells. Cadherin proteins have been found to play an important role in maintaining cytoskeletal structures (Tsukita et al., 1992), and in sensory cells, the increased Cdh1 immunoreactivity is spatially close to the site of actin, the cuticular plates of the cells. We have previously demonstrated rapid degradation of F-actin protein in the early phase of acute sensory cell apoptosis (Hu et al., 2002a). Together, this evidence suggests the involvement of Cdh1 in sensory cell degeneration.

We have also demonstrated the involvement of immunoglobulin superfamily and integrin family genes in acoustic trauma. *Icam1,* an immunoglobulin gene, is upregulated in both the apical and the basal partitions of the sensory epithelium, and its expression has previously been linked to the inflammatory response (Fujimoto et al., 2008; Glushakova et al., 2008), including cochlear inflammation (Suzuki and Harris, 1995). In ischemia/reperfusion models, early *Icam-1* expression has been observed (Olanders et al., 2002) and this expression has been linked to oxidative stress (Lange et al., 2008). Given the reduction in antioxidant capacity during noise trauma (Henderson et al., 2006), we argue that the increase in *Icam1* expression may be linked to oxidative stress in the cochlea.

In summary, the current study was designed to investigate the involvement of adhesion-related genes in cochlear pathogenesis caused by acoustic trauma. This study, for the first time, examined site-specific gene expression patterns in the sensory epithelia in noise-injured cochleae. We describe multiple novel findings, including constitutive expression

patterns of adhesion-related genes in normal rat cochleae and differential expression changes following acoustic trauma. Importantly, we uncover links between functional loss of the cochlea and gene expression changes. This study has implications for understanding of the molecular mechanisms of acute sensory cell damage and individual variation in cochlear susceptibility to acoustic overstimulation. Future investigations into the roles for these genes in the functional integrity of particular types of intercellular junctions in the cochlea will provide a better understanding of their contribution to noise-induced cochlear damage.

Supplementary Material

Refer to Web version on PubMed Central for supplementary material.

Acknowledgments

The research was supported by NIDCD1R01 DC010154-01 to BH Hu.

Abbreviation

ABR	Auditory brainstem response
SAM	Significance Analysis of Microarrays
PBS	phosphate buffered saline

References

Anderson JM, Van Itallie CM. Tight junctions and the molecular basis for regulation of paracellular permeability. Am J Physiol. 1995; 269:G467–75. [PubMed: 7485497]

Bahloul A, et al. Vezatin, an integral membrane protein of adherens junctions, is required for the sound resilience of cochlear hair cells. EMBO Mol Med. 2009; 1:125–38. [PubMed: 20049712]

Barshishat M, et al. Butyrate regulates E-cadherin transcription, isoform expression and intracellular position in colon cancer cells. Br J Cancer. 2000; 82:195–203. [PubMed: 10638989]

Bohne BA, et al. Cochlear damage following interrupted exposure to high-frequency noise. Hear Res. 1987; 29:251–64. [PubMed: 3305456]

Chen M, Geng JG. P-selectin mediates adhesion of leukocytes, platelets, and cancer cells in inflammation, thrombosis, and cancer growth and metastasis. Arch Immunol Ther Exp (Warsz). 2006; 54:75–84. [PubMed: 16648968]

Davies D, Holley MC. Differential expression of alpha 3 and alpha 6 integrins in the developing mouse inner ear. J Comp Neurol. 2002; 445:122–32. [PubMed: 11891657]

Engstrom H, Engstrom B. Structural changes in the cochlea following overstimulation by noise. Acta Otolaryngol Suppl. 1979; 360:75–9. [PubMed: 287359]

Fechter LD, et al. Cochlear protection from carbon monoxide exposure by free radical blockers in the guinea pig. Toxicol Appl Pharmacol. 1997; 142:47–55. [PubMed: 9007033]

Forge A, et al. Gap junctions and connexin expression in the inner ear. Novartis Found Symp. 1999; 219:134–50. discussion 151–6. [PubMed: 10207902]

Forge A, Schacht J. Aminoglycoside antibiotics. Audiol Neurootol. 2000; 5:3–22. [PubMed: 10686428]

Fredelius L, Rask-Andersen H. The role of macrophages in the disposal of degeneration products within the organ of corti after acoustic overstimulation. Acta Otolaryngol. 1990; 109:76–82. [PubMed: 2309562]

Frisch SM. Anoikis. Methods Enzymol. 2000; 322:472–9. [PubMed: 10914040]

Frisch SM, Francis H. Disruption of epithelial cell-matrix interactions induces apoptosis. J Cell Biol. 1994; 124:619–26. [PubMed: 8106557]

Frisch SM, Screaton RA. Anoikis mechanisms. Curr Opin Cell Biol. 2001; 13:555–62. [PubMed: 11544023]

Fujimoto K, et al. Early induction of moderate hypothermia suppresses systemic inflammatory cytokines and intracellular adhesion molecule-1 in rats with caerulein-induced pancreatitis and endotoxemia. Pancreas. 2008; 37:176–81. [PubMed: 18665080]

Glushakova O, et al. Fructose induces the inflammatory molecule ICAM-1 in endothelial cells. J Am Soc Nephrol. 2008; 19:1712–20. [PubMed: 18508964]

Grailer JJ, et al. L-selectin: role in regulating homeostasis and cutaneous inflammation. J Dermatol Sci. 2009; 56:141–7. [PubMed: 19889515]

Grossmann J. Molecular mechanisms of “detachment-induced apoptosis--Anoikis”. Apoptosis. 2002; 7:247–60. [PubMed: 11997669]

Gulley RL, Reese TS. Intercellular junctions in the reticular lamina of the organ of Corti. J Neurocytol. 1976; 5:479–507. [PubMed: 993823]

Guthrie JL, et al. Use of Bordetella pertussis BP3385 to establish a cutoff value for an IS481-targeted real-time PCR assay. J Clin Microbiol. 2008; 46:3798–9. [PubMed: 18784312]

Haga T, et al. Role of E-cadherin in the induction of apoptosis of HPV16-positive CaSki cervical cancer cells during multicellular tumor spheroid formation. Apoptosis. 2008; 13:97–108. [PubMed: 17906929]

Hamernik RP, et al. Anatomical correlates of impulse noise-induced mechanical damage in the cochlea. Hear Res. 1984; 13:229–47. [PubMed: 6735931]

Henderson D, et al. The Role of Oxidative Stress in Noise-Induced Hearing Loss. Ear Hear. 2006; 27:1–19. [PubMed: 16446561]

Henderson D, Hamernik RP. Impulse noise: critical review. J Acoust Soc Am. 1986; 80:569–84. [PubMed: 3745686]

Hirose K, et al. Mononuclear phagocytes migrate into the murine cochlea after acoustic trauma. J Comp Neurol. 2005; 489:180–94. [PubMed: 15983998]

Hu BH, Cai Q. Acoustic overstimulation modifies Mcl-1 expression in cochlear sensory epithelial cells. J Neurosci Res. 2010; 88:1812–21. [PubMed: 20091770]

Hu BH, et al. Differential expression of apoptosis-related genes in the cochlea of noise-exposed rats. Neuroscience. 2009; 161:915–925. [PubMed: 19348871]

Hu BH, et al. F-actin cleavage in apoptotic outer hair cells in chinchilla cochleas exposed to intense noise. Hear Res. 2002a; 172:1–9. [PubMed: 12361861]

Hu BH, et al. Involvement of apoptosis in progression of cochlear lesion following exposure to intense noise. Hear Res. 2002b; 166:62–71. [PubMed: 12062759]

Hu BH, et al. Extremely rapid induction of outer hair cell apoptosis in the chinchilla cochlea following exposure to impulse noise. Hear Res. 2006; 211:16–25. [PubMed: 16219436]

Hu, BH.; Zheng, G. Exposure to intense noise causes paracellular permeability of supporting cells in the organ of Corti. MidWinter Meeting of Assoc. Res. Otolaryngol; Phoenix, Arizona. 2008.

Hunter-Duvar I. Inner ear correlates in acoustic trauma. Trans Sect Otolaryngol Am Acad Ophthalmol Otolaryngol. 1977; 84:422.

Jamesdaniel S, et al. Noise induced changes in the expression of p38/MAPK signaling proteins in the sensory epithelium of the inner ear. J Proteomics. 2011 in press.

Kikuchi T, et al. Gap junctions in the rat cochlea: immunohistochemical and ultrastructural analysis. Anat Embryol (Berl). 1995; 191:101–18. [PubMed: 7726389]

Kikuchi T, et al. Gap junction systems in the mammalian cochlea. Brain Res Brain Res Rev. 2000; 32:163–6. [PubMed: 10751665]

Lange V, et al. Heterotopic rat heart transplantation (Lewis to F344): early ICAM-1 expression after 8 hours of cold ischemia. J Heart Lung Transplant. 2008; 27:1031–5. [PubMed: 18765197]

Leckband D, Prakasam A. Mechanism and dynamics of cadherin adhesion. Annu Rev Biomed Eng. 2006; 8:259–87. [PubMed: 16834557]

Leonova EV, Raphael Y. Organization of cell junctions and cytoskeleton in the reticular lamina in normal and ototoxically damaged organ of Corti. Hear Res. 1997; 113:14–28. [PubMed: 9387983]

Lim DJ. Ultrastructural cochlear changes following acoustic hyperstimulation and ototoxicity. Ann Otol Rhinol Laryngol. 1976; 85:740–51. [PubMed: 999139]

Lim DJ, Melnick W. Acoustic damage of the cochlea. A scanning and transmission electron microscopic observation. Arch Otolaryngol. 1971; 94:294–305. [PubMed: 5098718]

Lipscomb DM, et al. The effect of high level sound on hearing sensitivity, cochlear sensorineuroepithelium and vasculature of the chinchilla. Acta Otolaryngol. 1977; 84:44–56. [PubMed: 899752]

Littlewood Evans A, Muller U. Stereocilia defects in the sensory hair cells of the inner ear in mice deficient in integrin alpha8beta1. Nat Genet. 2000; 24:424–8. [PubMed: 10742111]

Malik RK. Regulation of apoptosis by integrin receptors. J Pediatr Hematol Oncol. 1997; 19:541–5. [PubMed: 9407943]

Meyerzum Gottesberge AM, et al. Inner ear defects and hearing loss in mice lacking the collagen receptor DDR1. Lab Invest. 2008; 88:27–37. [PubMed: 18026164]

Muller M. Frequency representation in the rat cochlea. Hear Res. 1991; 51:247–54. [PubMed: 2032960]

Nadol JB Jr. Intercellular junctions in the organ of Corti. Ann Otol Rhinol Laryngol. 1978; 87:70–80. [PubMed: 23719]

Nickel R, Forge A. Gap junctions and connexins in the inner ear: their roles in homeostasis and deafness. Curr Opin Otolaryngol Head Neck Surg. 2008; 16:452–7. [PubMed: 18797288]

Nunes FD, et al. Distinct subdomain organization and molecular composition of a tight junction with adherens junction features. J Cell Sci. 2006; 119:4819–27. [PubMed: 17130295]

Olanders K, et al. The effect of intestinal ischemia and reperfusion injury on ICAM-1 expression, endothelial barrier function, neutrophil tissue influx, and protease inhibitor levels in rats. Shock. 2002; 18:86–92. [PubMed: 12095141]

Pouyatos B, et al. Selective vulnerability of the cochlear Basal turn to acrylonitrile and noise. J Toxicol. 2009:908596. [PubMed: 20130768]

Pye A. Acoustic trauma effects with varying exposure times. Arch Otorhinolaryngol. 1981; 230:265–71. [PubMed: 7023441]

Raphael Y, Altschuler RA. Reorganization of cytoskeletal and junctional proteins during cochlear hair cell degeneration. Cell Motil Cytoskeleton. 1991; 18:215–27. [PubMed: 1711932]

Riazuddin S, et al. Tricellulin is a tight-junction protein necessary for hearing. Am J Hum Genet. 2006; 79:1040–51. [PubMed: 17186462]

Rossi B, Constantin G. Anti-selectin therapy for the treatment of inflammatory diseases. Inflamm Allergy Drug Targets. 2008; 7:85–93. [PubMed: 18691137]

Saunders JC, et al. The anatomical consequences of acoustic injury: A review and tutorial. J Acoust Soc Am. 1985; 78:833–60. [PubMed: 4040933]

Schneeberger EE, Lynch RD. Structure, function, and regulation of cellular tight junctions. Am J Physiol. 1992; 262:L647–61. [PubMed: 1616050]

Sha SH, et al. Differential vulnerability of basal and apical hair cells is based on intrinsic susceptibility to free radicals. Hear Res. 2001; 155:1–8. [PubMed: 11335071]

Shi X, Nuttall AL. Expression of adhesion molecular proteins in the cochlear lateral wall of normal and PARP-1 mutant mice. Hear Res. 2007; 224:1–14. [PubMed: 17184942]

Simonneau L, et al. Comparative expression patterns of T-, N-, E-cadherins, beta-catenin, and polysialic acid neural cell adhesion molecule in rat cochlea during development: implications for the nature of Kolliker's organ. J Comp Neurol. 2003; 459:113–26. [PubMed: 12640664]

Stamenkovic I. The L-selectin adhesion system. Curr Opin Hematol. 1995; 2:68–75. [PubMed: 9371974]

Suzuki M, Harris JP. Expression of intercellular adhesion molecule-1 during inner ear inflammation. Ann Otol Rhinol Laryngol. 1995; 104:69–75. [PubMed: 7530436]

Thorne PR, Gavin JB. Changing relationships between structure and function in the cochlea during recovery from intense sound exposure. Ann Otol Rhinol Laryngol. 1985; 94:81–6. [PubMed: 3970508]

Thorne PR, et al. A quantitative study of the sequence of topographical changes in the organ of Corti following acoustic trauma. Acta Otolaryngol. 1984; 97:69–81. [PubMed: 6689831]

Tian G, et al. Clarin-1, encoded by the Usher Syndrome III causative gene, forms a membranous microdomain: possible role of clarin-1 in organizing the actin cytoskeleton. J Biol Chem. 2009; 284:18980–93. [PubMed: 19423712]

Toyama K, et al. Expression of the integrin genes in the developing cochlea of rats. Hear Res. 2005; 201:21–6. [PubMed: 15721557]

Tsukita S, et al. Molecular linkage between cadherins and actin filaments in cell-cell adherens junctions. Curr Opin Cell Biol. 1992; 4:834–9. [PubMed: 1419062]

Tsuprun V, Santi P. Ultrastructure and immunohistochemical identification of the extracellular matrix of the chinchilla cochlea. Hear Res. 1999; 129:35–49. [PubMed: 10190750]

Tusher VG, et al. Significance analysis of microarrays applied to the ionizing radiation response. Proc Natl Acad Sci U S A. 2001; 98:5116–21. [PubMed: 11309499]

Vandesompele J, et al. Accurate normalization of real-time quantitative RT-PCR data by geometric averaging of multiple internal control genes. Genome Biol. 2002; 3:RESEARCH0034. [PubMed: 12184808]

Wagner W, et al. Noise in magnetic resonance imaging: no risk for sensorineural function but increased amplitude variability of otoacoustic emissions. Laryngoscope. 2003; 113:1216–23. [PubMed: 12838022]

Weston MD, et al. MicroRNA-183 family expression in hair cell development and requirement of microRNAs for hair cell maintenance and survival. Dev Dyn. 2011; 240:808–19. [PubMed: 21360794]

Whitlon DS. E-cadherin in the mature and developing organ of Corti of the mouse. J Neurocytol. 1993; 22:1030–8. [PubMed: 8106878]

Whitlon DS, Rutishauser US. NCAM in the organ of Corti of the developing mouse. J Neurocytol. 1990; 19:970–7. [PubMed: 2292721]

Whitlon DS, et al. A temporospatial map of adhesive molecules in the organ of Corti of the mouse cochlea. J Neurocytol. 1999; 28:955–68. [PubMed: 10900097]

Wilcox ER, et al. Mutations in the gene encoding tight junction claudin-14 cause autosomal recessive deafness DFNB29. Cell. 2001; 104:165–72. [PubMed: 11163249]

Yang WP, et al. Quantitative analysis of apoptotic and necrotic outer hair cells after exposure to different levels of continuous noise. Hear Res. 2004; 196:69–76. [PubMed: 15464303]

Research Highlights

- Multiple families of adhesion-related genes are expressed in the rat cochlea.
- Acoustic trauma alters expression patterns of adhesion-related genes.
- Cochlear functional loss is related to the expression levels of adhesion genes.
- Genes showing expression changes exhibit diverse constitutive expression levels

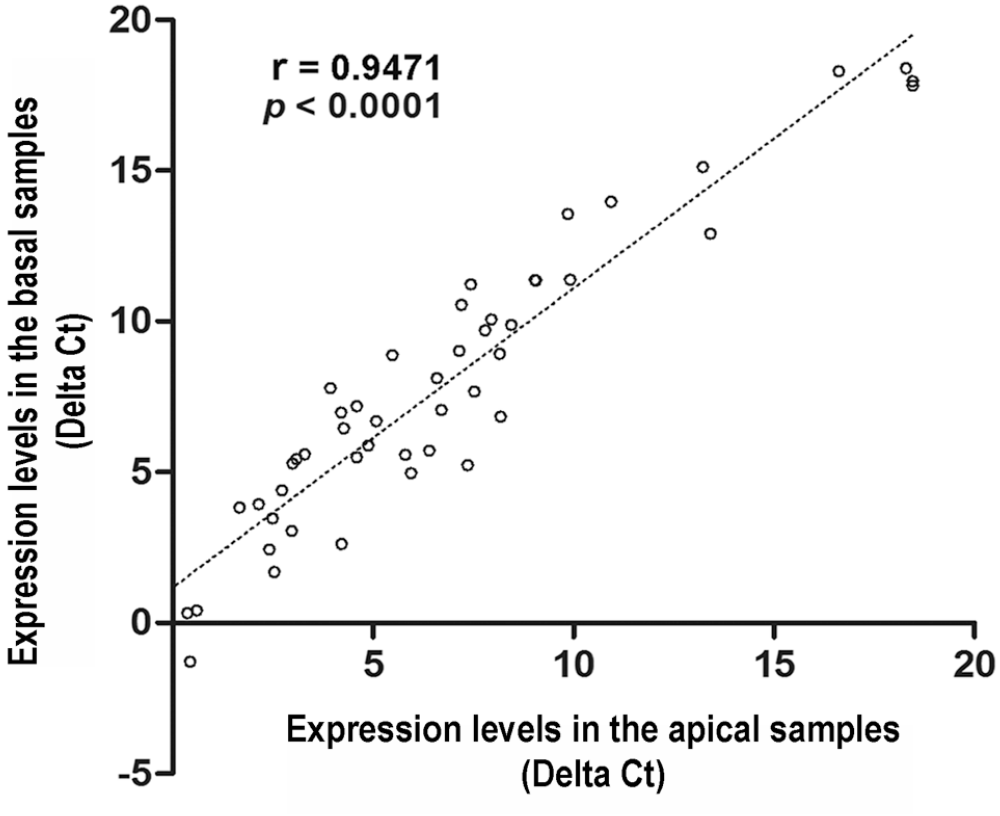

Figure 1.
Scatter plot showing the relative expression level (ΔCt) of each adhesion-related gene in the apical samples versus the basal samples. Expression levels were normalized to the reference genes. Correlation coefficients (r) and *p* values were determined with a Pearson's correlation test.

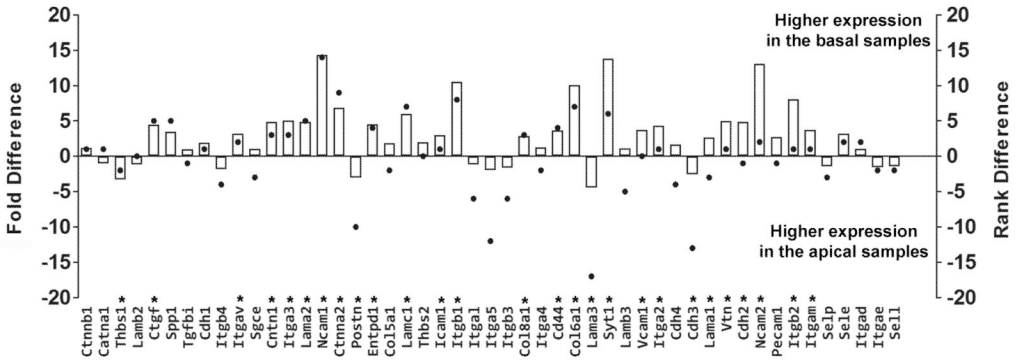

Figure 2.

Comparisons of the expression levels of adhesion-related genes between apical and basal samples. The expression levels of the genes in the apical samples are plotted as the baseline value (the zero line). Bars represent the fold differences between the basal and apical expression levels, and dots represent the rank difference between the apical and basal expression levels. A positive value indicates higher expression of a gene in the basal samples, and a negative value represents higher expression of a gene in the apical samples. Asterisks mark the genes having a fold difference equal to or greater than 2 and *q*-values less than or equal to 0.01.

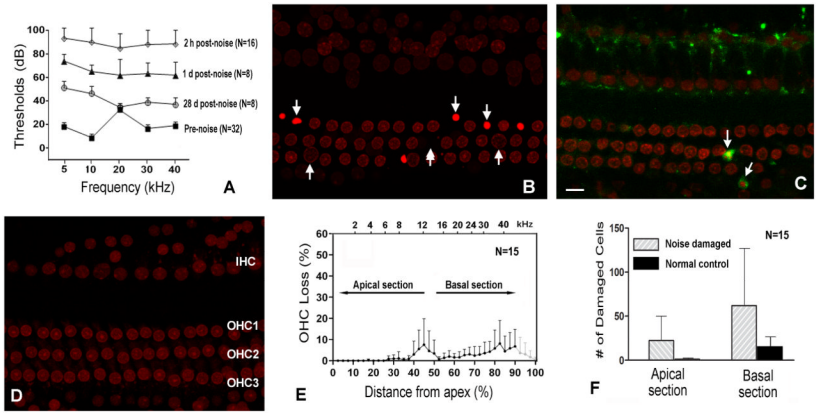

Figure 3.

Functional and pathological changes in the noise-traumatized cochleae. *A*, The threshold shifts of auditory brainstem responses (ABRs) at 2 h, 1 day, and 28 days post-exposure. *B*, An example of sensory cell damage illustrated by propidium iodide staining from a cochlea examined at 2 h post-noise exposure. Arrows indicate sensory cells with malformed nuclei. The double-arrow indicates the site of a missing cell. *C*, An example of caspase-3 staining from a cochlea examined at 2 h post-noise exposure. Arrows indicate the sensory cells having condensed or fragmented nuclei. These cells exhibit strong caspase-3 activity (green). Scale bar = 20 μm. *D*, An example of the nuclear morphology in a normal sensory epithelium from a control ear. IHC indicates inner hair cells, while OHC1, OHC2, and OHC3 indicate the first, second, and third rows of outer hair cells, respectively. *E*, Cochleogram showing the distribution of damaged sensory cells in the organ of Corti at 2 h post-noise exposure. The two horizontal arrows mark the regions of the sensory epithelium used for quantification of sensory cell damage in the apical and basal sections (see Fig. 3F). Noted that the counts from the basal region between 90–100% were not included in the calculation for Fig. 3F. *F*, Comparison of the numbers of degenerated sensory cells in the apical and basal sections of the sensory epithelium in normal and noise-damaged ears. The number of damaged sensory cells in the basal section is significantly higher than in the apical section (paired Student's t test, $*p < 0.05$). Bars: one standard deviation. N = the number of the ears.

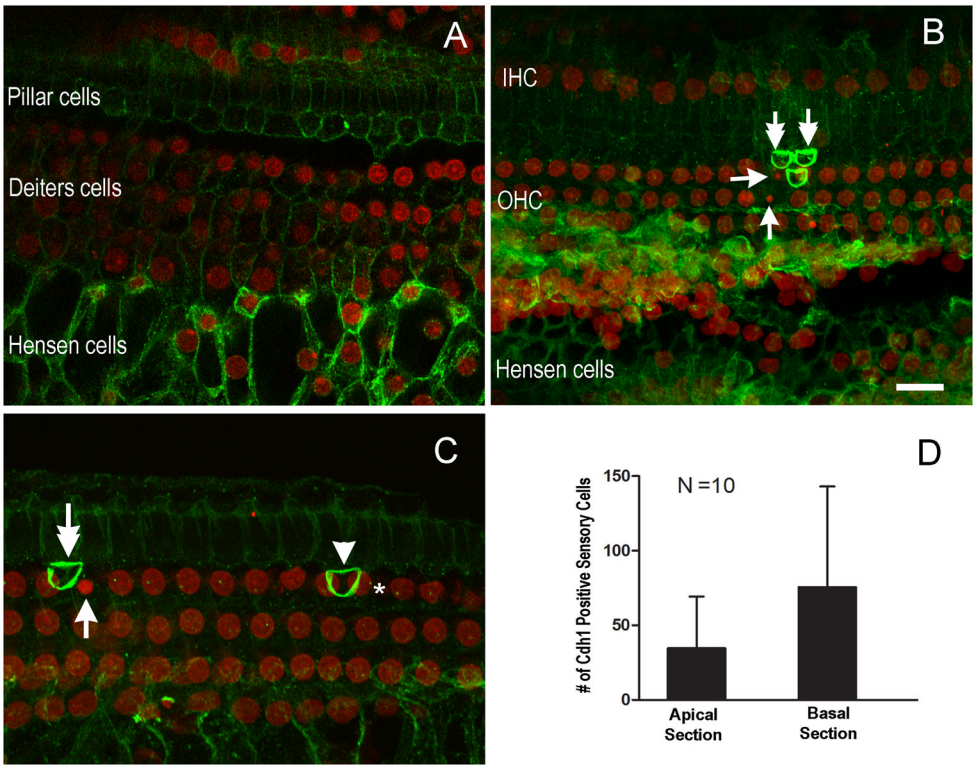

Figure 4.

Cdh1 immunoreactivity in the sensory epithelium of a normal and a noise-traumatized cochlea. *A*, A micrograph showing distribution of Cdh1 immunoreactivity in a normal organ of Corti. The Cdh1 immunoreactivity (green fluorescence) is located in the intercellular junctions between supporting cells, including pillar cells, Deiters cells, and Hensen cells. The nuclei of the cells, illustrated by propidium iodide staining (red fluorescence), appear normal. *B and C*, Cdh1 staining in a noise-traumatized organ of Corti. Some outer hair cells exhibit strong Cdh1 immunoreactivity in their top junctions with neighboring supporting cells (double-arrows) along with malformed nuclei (arrows). One OHC has strong Cdh1 immunoreactivity (the arrowhead in C), but its nucleus has a relatively normal shape (see the nucleus to the left of the asterisk). IHC represents inner hair cells, while OHC represents outer hair cells. Scale bar = 20 μm. *D*, Comparison of the numbers of Cdh1-positive sensory cells between the apical and the basal sections of the sensory epithelium. The basal section has more Cdh1-positive sensory cells than the apical section (paired Student's t test, * $p < 0.01$). Bars: one standard deviation. N = the number of ears.

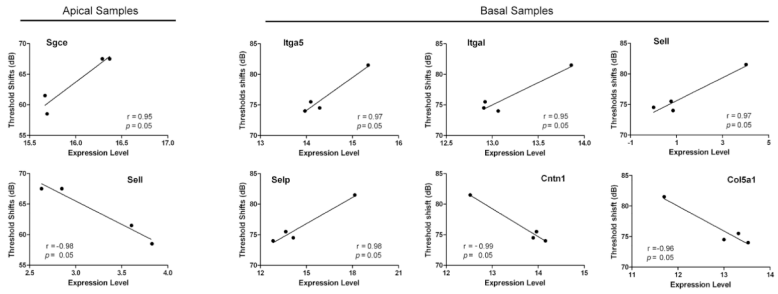

Figure 5.
Correlations between the threshold shifts of auditory brainstem responses (ABRs) and the relative expression levels of seven adhesion-related genes from either apical or basal samples.

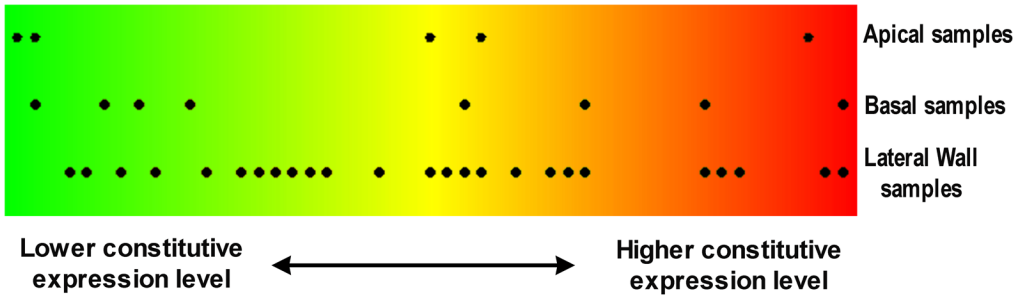

Figure 6.
The distribution of genes showing expression changes along the rank sequence of the 49 genes examined. Dots indicate the individual ranking position of the genes based on their constitutive expression levels.

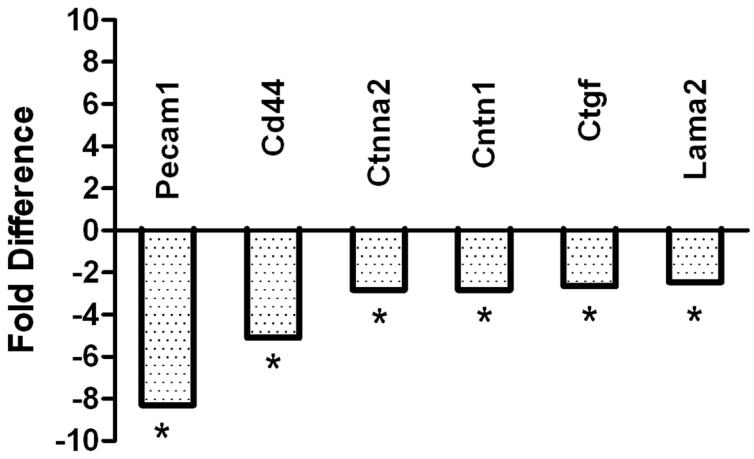

Figure 7.

Fold difference of the transcriptional expression levels of adhesion-related genes between normal tissues and noise-damaged tissues examined 1 day post-exposure. Negative values indicate the downregulation of genes. Asterisks indicate *q*-values < 0.01.

Table 1

The 49 adhesion-related genes examined.

GenBank	Symbol	Name
NM_001007145	Catna1	Catenin (cadherin associated protein), alpha 1
NM_053357	Ctnnb1	Catenin (cadherin associated protein), beta 1
NM_031333	Cdh2	Cadherin 2
XM_001061943	Cdh4	Cadherin 4
XM_215375	Col6a1	Collagen, type VI, alpha 1
NM_012967	Icam1	Intercellular adhesion molecule 1
NM_031521	Ncam1	Neural cell adhesion molecule 1
NM_031591	Pecam1	Platelet/endothelial cell adhesion molecule 1
XM_340884	Itga3	Integrin alpha 3
XM_235707	Itga5	Integrin alpha 5 (fibronectin receptor alpha)
NM_031768	Itgae	Integrin, alpha E, epithelial-associated
NM_012711	Itgam	Integrin alpha M
NM_017022	Itgb1	Integrin beta 1 (fibronectin receptor beta)
NM_153720	Itgb3	Integrin beta 3
XM_237536	Lama1	Laminin, alpha 1
XM_226159	Lama3	Laminin, alpha 3
XM_223087	Lamb3	Laminin, beta 3
NM_022266	Ctgf	Connective tissue growth factor
NM_057118	Cntn1	Contactin 1
XM_573983	Tgfbi	Transforming growth factor, beta induced
NM_012924	Cd44	Cd44 molecule
NM_001002023	Sgce	Sarcoglycan, epsilon
NM_138879	Sale	Selectin, endothelial cell
NM_013114	Selp	Selectin, platelet
XM_214778	Thbs2	Thrombospondin 2
XM_232077	Ctnna2	Catenin (cadherin associated protein), alpha 2
NM_031334	Cdh1	Cadherin1
XM_226426	Cdh3	Cadherin 3, type 1, P-cadherin (placental)
NM_134452	Col5a1	Collagen, type V, alpha 1
XM_221536	Col8a1	Collagen, type VIII, alpha 1
NM_012889	Vcam1	Vascular cell adhesion molecule 1
NM_203409	Ncam2	Neural cell adhesion molecule 2
XM_345156	Itga2	Integrin, alpha 2
XM_230033	Itga4	Integrin alpha 4
NM_031691	Itgad	Integrin, alpha D
NM_001033998	Itgal	Integrin alpha L
XM_230950	Itgav	Integrin alpha V
XM_001069791	Itgb2	Integrin beta 2
NM_013180	Itgb4	Integrin beta 4

GenBank	Symbol	Name
XM_219866	Lama2	Laminin, alpha 2
NM_012974	Lamb2	Laminin, beta 2
XM_341133	Lamc1	Laminin, gamma 1
NM_012881	Spp1	Secreted phosphoprotein 1
XM_342245	Postn	Periostin, osteoblast spedfic factor
NM_019156	Vtn	Vitronectin
NM_001033680	Syt1	Synaptotagmin I
NM_019177	Sell	Selectin, lymphocyte
NM_001013062	Thbsl	Thrombospondin 1
NM_022587	Entpd1	Ectonucleoside triphosphate diphosphohydrolase 1

Table 2

Differential expression of adhesion-related genes 2 h post-exposure in the apical and basal sections. *q* value <0.01 indicates a significant expression change.

Symbol	Apical Section		Basal Section	
	Fold change	*q* value	Fold change	*q* value
Itgae	6.464	<0.01		
Sell	6.233	<0.01		
Itga5	2.063	<0.01		
* Icam1	4.112	<0.01	8.206	<0.01
* Thbs1	4.765	<0.01	2.241	<0.01
Selp			376.5	<0.01
Sele			18.79	<0.01
Itgb2			13.35	<0.01
Itga3			3.180	<0.01
Cdh1			2.457	<0.01
Cdh2			3.191	<0.01

Note: asterisks indicate the genes that are altered in both the apical and the basal sections

Table 3

Differential expression of adhesion-related genes 2 h post-exposure in the lateral wall tissues. *q* value <0.01 indicates a significant expression change.

	Genes	Fold change	*q* value
Upregulated	Thbs1	7.464	<0.01
	Selp	107.3	= 0.01
	Cdh3	2.799	= 0.01
	Sele	6.600	= 0.01
	Ncam1	8.442	<0.01
	Lama2	5.260	<0.01
	Spp1	5.408	<0.01
	Itga4	3.850	<0.01
	Thbs2	2.694	<0.01
	Ncam2	8.770	<0.01
	Itgav	3.986	<0.01
	Lama1	5.306	<0.01
	Syt1	11.94	<0.01
	Cntn1	3.938	<0.01
Down regulated	Lamb 3	3.891	<0.01
	Col8a1	7.198	<0.01
	Cdh2	3.965	<0.01
	Entpd1	4.651	<0.01
	Lamc1	5.269	<0.01
	Itgb1	4.431	<0.01
	Vtn	7.438	<0.01
	Ctnna2	2.814	<0.01
	Vcam1	4.250	<0.01
	Col6a1	3.713	<0.01
	Itga2	2.374	= 0.01